INTERNATIONAL JOURNAL OF CLIMATOLOGY, VOL. 16, 243–264 (1996)

CERTAIN SEASONAL CHARACTERISTIC FEATURES OF OCEANIC HEAT BUDGET COMPONENTS OVER THE INDIAN SEAS IN RELATION TO THE SUMMER MONSOON ACTIVITY OVER INDIA

U. C. MOHANTY* AND K. J. RAMESH
Centre for Atmospheric Sciences, Indian Institute of Technology, Delhi, Hauz Khas, New Delhi - 110 016, India

AND

M. C. PANT
India Meteorological Department, Lodi Road, New Delhi - 110 003, India

Received 22 May 1994
Accepted 25 May 1995

ABSTRACT

The present study has been undertaken to examine the oceanic heat budget components and their variability over the Indian seas in relation to the extreme monsoon activity (flood/drought) over the Indian subcontinent. For this purpose, various components of oceanic heat budget have been analysed for pre-monsoon (March–May), monsoon (June–September), post-monsoon (October–December) and winter (January–February) seasons over India. The data base used in this study consists of mean monthly marine meteorological fields for 30 years (1950–1979), which is a part of the Comprehensive Ocean Atmosphere Data Set (COADS) analysed at 1° latitude by 1° longitude resolution.

The mean fields of incoming shortwave radiation flux over the Indian seas in different seasons vary in accordance to the sun's position and cloud cover variations. The latent heat flux undergoes considerable seasonal variations, particularly over the Arabian Sea. There is a dominance of latent heat flux (representing the oceanic heat loss) over shortwave solar flux (representing the oceanic heat gain) during the monsoon season, which results in a zone of net oceanic heat loss over the central Arabian Sea. This feature produces a positive feedback for the maintenance of deep cumulus convection over the Arabian Sea in this season.

It is also found that oceanic heat budget components over the Indian seas exhibit significant variability in relation to the extreme monsoon activity leading to flood/drought over India. Based on the above analysis, mean monthly variations of the oceanic heat budget components over three smaller sectors of the Indian seas, namely west equatorial Indian Ocean, Arabian Sea and Bay of Bengal, are also examined. The variations are found to be considerably different between the two extreme categories of the monsoon. It becomes evident from this study that the oceanic sectors of west equatorial Indian Ocean and Bay of Bengal experience a large reduction of net heat flux from April to May prior to a flood monsoon season over India. This suggests that a spectacular increase of latent heat flux and decrease of shortwave flux occurs over these oceanic sectors, leading to a sharp reduction of net heat flux.

KEY WORDS: variability of atmosphere-ocean; oceanic heat budget; summer monsoon; air–sea interaction; student *t*-test; Indian seas

INTRODUCTION

The Indian summer monsoon is a large-scale circulation system that develops every year over the Indian Ocean during the middle of May and continues until the end of September. The tropical oceanic regions, in particular, the Arabian Sea, the Bay of Bengal, and the Indian Ocean act as main reservoirs of heat and moisture in supplying the necessary energy to maintain the large-scale monsoon circulation and its associated activity over the Indian subcontinent. Therefore, it is important to study the air–sea interaction processes over the tropical areas of the Indian seas and the variability of the oceanic heat fluxes in relation to the summer monsoon activity over India. Incidentally, these fluxes are not measured directly, owing to

* Present affiliation: National Centre for Medium Range Weather Forecasting, Mausam Bhawan Complex, Lodi Road, New Delhi - 110 003, India.

CCC 0899-8418/96/030243–22

lack of adequate observations over the Indian seas to estimate them, but a few observational studies (Pisharoty, 1965; Das, 1983; Mohanty *et al.*, 1983; Mohanty and Mohan Kumar, 1990; and others) are found in the literature based on the data collected during IIOE, ISMEX-72, MONSOON-77 and MONEX-79 experiments. These studies have demonstrated the importance of the energy fluxes over the Indian seas during different epochs of the summer monsoon activity over India.

Several investigations have been carried out to establish a possible relationship between sea-surface temperature (SST) variations over the Indian seas and monsoon activity over the Indian subcontinent (Shukla, 1975, 1987; Weare, 1979; Rao and Goswamy, 1988; and others). Recent studies using long-term marine meteorological analyses (Mohanty and Ramesh, 1993) indicate that ocean surface parameters, such as SST and sea-level pressure, do not display any significant variability over the Indian seas. On the other hand the parameters that determine the flux transfer of heat and moisture from the ocean surface and the atmosphere, such as wind, cloud, and humidity exhibit significant variability over the Indian seas between the extreme categories of the monsoon (flood and drought). As the interaction between the atmosphere and ocean takes place through the exchange of heat, moisture, and momentum, it is relevant to study the linkage between the air–sea fluxes and monsoon activity rather than the SST anomaly and the monsoon activity (Mohanty *et al.*, 1994). Further, these fluxes serve as a lower boundary condition for the atmosphere and as an upper boundary for the ocean in driving the large-scale ocean–atmosphere coupled models (Manabe *et al.*, 1975).

The present study has undertaken the examination of the oceanic heat budget components during different seasons (pre-monsoon, monsoon, post-monsoon, and winter) in relation to monsoon activity over India by using mean monthly marine meteorological fields for a period of 30 years (1950–1979). Further, the variability of oceanic heat budget components during the extreme categories of the summer monsoon activity, namely large excess rainfall (flood) and large deficient rainfall (drought) years, over the Indian subcontinent are examined.

DATA SOURCES AND ANALYSIS PROCEDURE

As an outcome of the joint efforts of several organizations, namely National Oceanic and Atmospheric Administration (NOAA), National Climate Data Centre (NCDC), Cooperative Institute for Research in Environmental Sciences (CIRES), and National Centre for Atmospheric Research (NCAR), the Comprehensive Ocean–Atmosphere Data Set (COADS) was archived. For the first time, the most efficient and up-to-date techniques have been used to compile all available oceanic and atmospheric data over the world oceans (Fletcher *et al.*, 1983; Oort *et al.*, 1987). The COADS consists of mean monthly marine surface meteorological fields, compiled and checked for quality, collected by ships and analysed on 2° latitude by 2° longitude resolution from 1854 to 1979. The data used in the present study are the reanalysed analyses at 1° latitude by 1° longitude resolution at the Geophysical Fluid Dynamics Laboratory (GFDL), Princeton University, New Jersey, USA for a period of 30 years (1950–1979). A large number of studies have been carried out with this data in order to study the influence of oceans on the climate variability (Oort *et al.*, 1987; and others).

Following Bhalme and Jadhav (1984), based on the seasonal rainfall over India as a whole, 30 monsoon seasons (1950–1979) are classified into categories of flood, drought, and normal. Large deficient (excess) rainfall years are categorized depending on the percentage departure of the rainfall decrease (excess) by 10 per cent, which closely corresponds to one standard deviation of the long-term mean monsoon rainfall. Out of the 30 monsoon seasons considered, six were found to be flood years (1956, 1959, 1961, 1970, 1973, and 1975) and eight were found to be drought years (1951, 1952, 1965, 1966, 1968, 1972, 1974, and 1979). The remaining 16 years are considered in the category of normal monsoon years.

The domain of the study extends from 30°S to 30°N and 30°E to 110°E, which represents the major oceanic regions under the influence of the monsoon region. The important geographical regions covered in the analysis area are the Mascarene High, Tropical Indian Ocean, Somali coast, Arabian Sea, and Bay of Bengal. Broadly, the derived radiation and turbulent fluxes are analysed in this study for the four seasons, namely pre-monsoon (March–May), monsoon (June–September), post-monsoon (October–December), and winter (January–February), over the Indian seas. Further, the variability of these air–sea fluxes between the two extreme categories of the monsoon (flood and drought) is studied. The statistical significance of these differences (anomaly) fields between the two extreme categories of the monsoon is examined by using Student's *t*-test.

COMPUTATIONAL PROCEDURE

Net balance of the radiative and turbulent fluxes of heat and moisture at the air–sea interface accounts for the net oceanic heat gain/loss. The net oceanic heat budget equation can be written as

$$Q_N = Q_R - Q_B - Q_H - Q_E \tag{1}$$

where Q_N is the net heat flux, Q_R is the incoming shortwave radiation, Q_B is the effective outgoing longwave radiation, Q_H is the sensible heat flux, and Q_E is the latent heat flux.

Over the tropical oceans, among the various terms of equation (1), Q_R contributes significantly to the oceanic heat gain whereas other terms contribute towards heat loss from the oceanic surface. In this study, various heat budget components have been estimated in terms of the analysed surface marine meteorological fields over the Indian seas. Because the advection of heat maintains long-term balance on the climatic scale, its contribution is not considered in this study. The estimation procedures of various components of the oceanic heat budget are summarized below. The detailed computational procedure is given in the Appendix.

Incoming solar radiation flux (Q_R)

The major source of energy for most of the physical processes over the tropical oceans comes from the solar radiative flux reaching the ocean surface. Because direct measurements are rather sparse, Q_R is calculated by making use of available meteorological parameters at the ocean surface. A method proposed by Reed (1977) is adopted for the estimation of Q_R. Using the semi-empirical relationship suggested by Seckel and Beaudry (1973), the clear-sky radiation (Q_0) is evaluated. Subsequently, Q_0 is corrected for the transmission effects of shortwave solar flux through clouds and the noon altitude of the sun, following Reed (1977). Then, the net incoming shortwave flux is estimated following the sea-surface albedo factors suggested by Payne (1972).

Effective outgoing longwave radiation (Q_B)

Meteorological quantities, such as the SST, sea–air temperature difference, vapour pressure, and cloud cover, largely determine the Q_B going out of the sea surface. In general, Q_B does not exhibit any significant temporal and spatial variabilities and is found to be very small in magnitude over the tropical oceanic regions. Following the empirical relationship suggested by Giruduk and Malevski-Holekyich (1973), Q_B is estimated in this study and its estimates are found to give least errors during the summer monsoon season over the Indian seas (Mohanty, 1981; Mohanty and Mohan Kumar, 1991). Based on the formulae suggested by Egorov (1976), the effect of cloudiness is included in the estimation of Q_B. By using the statistical relationship suggested by Mohanty and Mohan Kumar (1991), which reduces the systematic errors between computed and measured fluxes of longwave radiation, Q_B is then estimated over the Indian seas.

Estimation of sensible and latent heat fluxes (Q_H and Q_E)

The turbulent exchange processes of heat and moisture across the air–sea interface are the most important factors over the tropical Indian seas. Among them, the turbulent exchange process of moisture largely determines the net oceanic heat gain/loss, because the Bowen's ratio over the tropical oceans is very small. Both Q_H and Q_E are estimated in this study by using bulk aerodynamic formulation based on temperature, moisture gradient, and wind speed at the air–sea interface. The exchange coefficients, which play a very important role in the turbulent transfer process, are estimated in this study as a function of wind speed and atmospheric stability (Mohanty and Mohan Kumar, 1990). The exchange coefficients thus computed compare well with the corresponding estimates of Bunker (1972) and Kondo and Akira (1975).

RESULTS AND DISCUSSION

In this section, mean fields of the significant oceanic heat budget components during the four seasons, namely pre-monsoon, monsoon, post-monsoon, and winter, over the Indian seas are analysed. Differences of oceanic heat budget components in the years of extreme monsoon activity (flood/drought) over the Indian seas are presented and discussed for different seasons, and their characteristic features are brought out. Besides the above, monthly variations of the dominant oceanic heat budget components in the flood and drought categories averaged over the three oceanic regions selected, namely the equatorial Indian Ocean (box 1), the Arabian Sea (box 2) and the Bay of Bengal (box 3), are also presented.

Distribution of mean fields of the oceanic heat budget components over the Indian seas

The mean fields of shortwave radiation flux (SWF), latent heat flux (LHF), and net oceanic heat flux (NHF) over the Indian seas in the pre-monsoon (March–May; MAM), monsoon (June–September; JJAS), post-monsoon (October–December; OND), and winter (January–February; JF) seasons over India are illustrated in Figures 1–3. Because the magnitudes of longwave flux (LWF) and sensible heat flux (SHF) are found to be considerably less as compared with those of SWF and LHF, the discussion of the results in this study is limited to the components of SWF, LHF, and NHF. However, it is to be noted that the contributions from LWF and SHF are included for the estimation of NHF.

Shortwave radiation flux. In the pre-monsoon season (Figure 1(a)), maximum shortwave radiation flux (SWF) is found over the north and central Arabian Sea sectors. The distribution of the flux depicts a stronger north–south gradient over the north Indian Ocean (Arabian Sea and Bay of Bengal) than over the south Indian Ocean. With the establishment of the summer monsoon (Figure 1(b)), the distribution of the SWF changes its orientation to the east–west direction. This change in the orientation of the SWF distribution could be attributed mainly to the prevailing east–west oriented cloud cover distribution over the Indian seas in association with south-westerly monsoon flow present over the oceanic areas to the north of the Equator. Large magnitudes of the SWF are found over the Somalia coast and off south Arabian Peninsula and lower magnitudes over the eastern Arabian Sea and Bay of Bengal. In the post-monsoon months (Figure 1(c)), the SWF distribution over the Indian seas shows higher magnitudes over the south Indian Ocean (south of 10°S) and lower magnitudes over the northern sector of the Arabian Sea and the Bay of Bengal. During the winter season (Figure 1(d)), minimum SWF magnitudes are found over the equatorial oceanic region and larger magnitudes of the flux on either side of the equatorial belt.

Latent heat flux. During the pre-monsoon period, a zone of high latent heat flux (LHF) is found over the south-western sector (0°–10°N) of the Arabian Sea, the Bay of Bengal and over the western Arabian Sea (Figure 2(a)). The zone of maximum LHF lies over the south Indian Ocean as well. During the monsoon season (Figure 2(b)), the LHF over the Arabian Sea and the Bay of Bengal shows a considerable increase. The zone of maximum LHF lies during this season over the south-western and central Arabian Sea, which generally coincides with the zone of the low-level wind maximum over the region during the monsoon months. The distribution of LHF in the post-monsoon season shows a significant decrease over the Indian seas as compared with that of the monsoon season (Figure 2(c)). However, a zone of high latent heat flux is

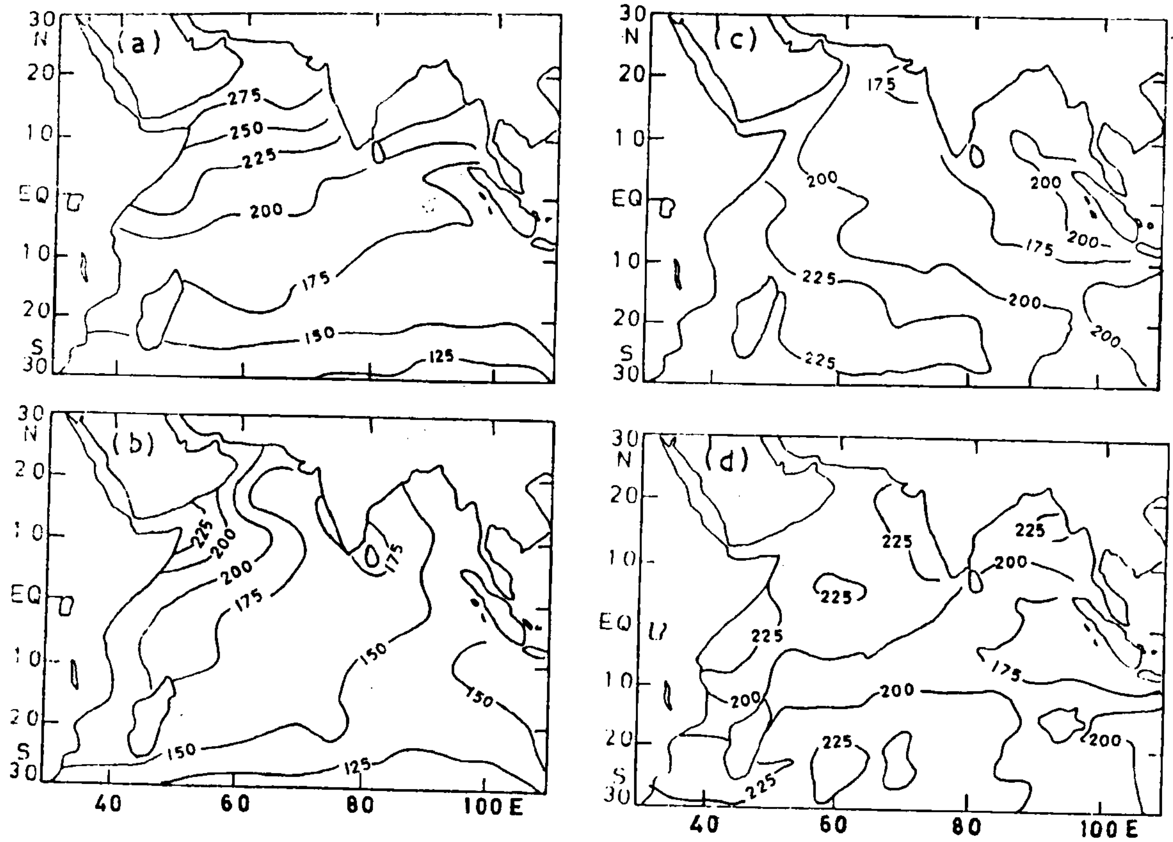

Figure 1. Distribution of mean short wave radiation flux over the Indian seas during different seasons (isopleth interval: 25 W m^{-2}). (a) Pre-monsoon; (b) monsoon; (c) post-monsoon; (d) winter

still observed over the south-west Arabian Sea during the post-monsoon period. Similar features of LHF distribution are also observed in the winter season (Figure 2(d)). It is of particular interest to note that the magnitudes of the LHF over the equatorial region of the Indian Ocean are comparatively small and remain nearly the same in all the four seasons.

Net oceanic heat flux. The distribution of net oceanic heat flux (NHF) over the Indian seas in the pre-monsoon season (Figure 3(a)) is characterized by a net heat gain over the region surrounded by 10°N–10°S latitudes. This indicates the dominance of the SWF over the LHF in the equatorial oceanic region. In the monsoon season (Figure 3(b)), the region of net heat loss lies over the central and eastern parts of the Arabian Sea, which nearly coincides with the zone of maximum LHF and reduced solar insolation due to cloud coverage in this season. The region to the south of 10°S is characterized by net heat loss in both the pre-monsoon and monsoon seasons. The NHF in the post-monsoon season shows a net gain over most parts of the Indian seas (Figure 3(c)), except over the south-eastern Indian Ocean, where there is a net heat loss from the ocean surface. The distribution of NHF in the winter season shows nearly similar features to that of the post-monsoon season, except that there is an enhanced zone of net heat gain over the Arabian Sea (Figure 3(d)). The magnitudes of LHF during winter are large over the Indian seas, due mainly to the prevailing surface winds (of the order of 5–8 m s^{-1}) though SST is of the order of 26–28°C. Further, these LHF magnitudes have good correspondence with the similar fields of Hastenrath and Lamb (1979).

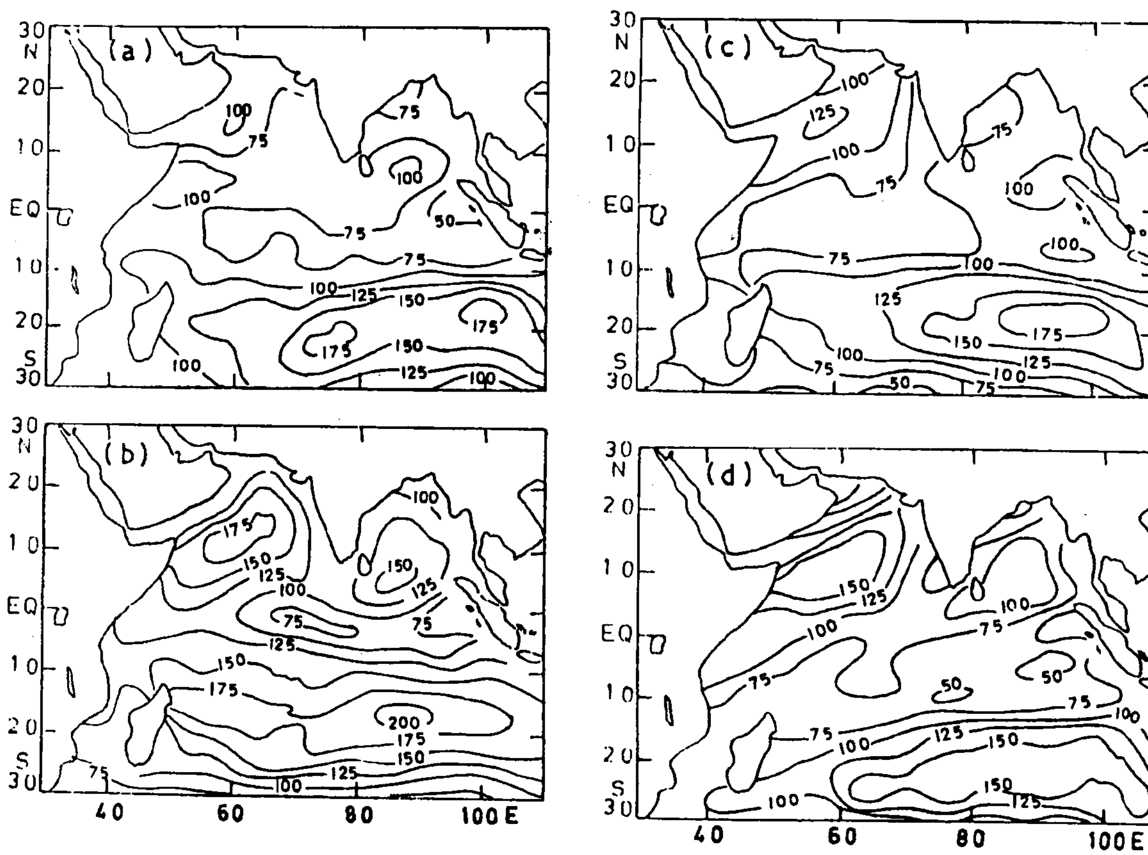

Figure 2. Same as Figure 1 but for latent heat flux (isopleth interval: 25 W m^{-2})

Seasonal variation of the dominant oceanic heat budget components between the extreme categories of the monsoon (flood/drought)

In this section, the difference fields of dominant oceanic heat budget componets—SWF, LHF and NHF—between the large excess (flood) and large deficient (drought) monsoon rainfall years over India have been examined for the pre-monsoon, monsoon, and post-monsoon seasons. As the anomaly fields of the heat budget components in the winter season do not depict any significant differences, these are not presented in this study.

Shortwave flux. The difference fields of the SWF, along with their corresponding statistically significant t-value distribution (hatched areas) for the pre-monsoon, monsoon and post-monsoon seasons, are presented in Figure 4.

During the period prior to flood monsoon years (Figure 4(a)), a considerable reduction is found in the incoming SWF by about 10–20 W m^{-2} over the Indian seas (15°N–15°S) covering largely the equatorial oceanic region, both the Arabian Sea and the Bay of Bengal. All of these negative flux difference regions are found to be significant statistically. Increase in cloud cover over these hatched areas during the pre-monsoon period prior to a flood monsoon season is considered to be mainly responsible for the significant decrease in the magnitude of SWF reaching the ocean surface over the Indian seas. Over the south Indian Ocean, however, small pockets of significant positive SWF differences are observed.

During the monsoon season, the zone of maximum significant negative SWF difference is found over the north and east Arabian Sea (Figure 4(b)). Besides this, few more significant negative SWF differences

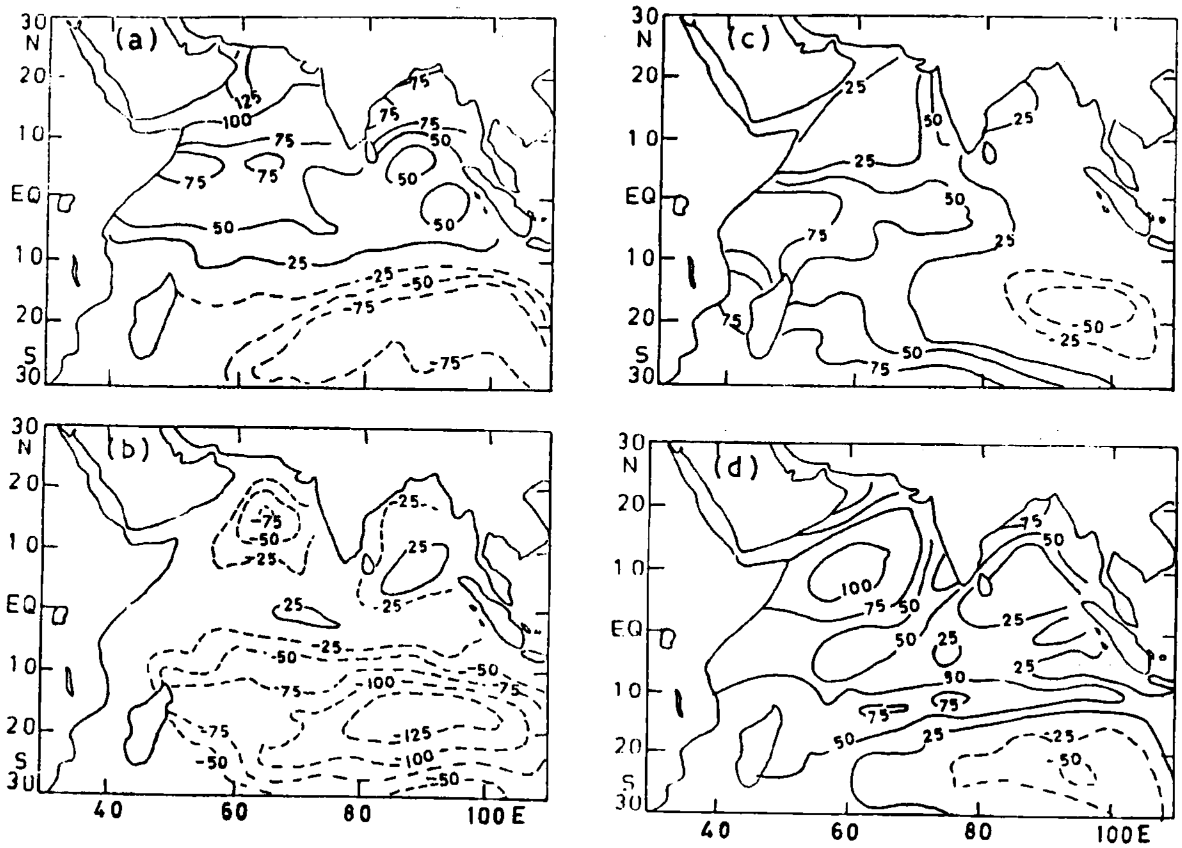

Figure 3. Same as Figure 1 but for net oceanic heat flux (Isopleth interval: 25 W m^{-2})

are observed over the oceanic areas off Sri Lanka, equatorial west Indian Ocean and the east coast of Africa adjoining Madagascar Island.

The difference fields of SWF in the post-monsoon seasons (Figure 4(c)) do not show any significant differences over large parts of the north Indian oceanic region. However, small pockets of significant SWF differences are observed over the central equatorial region of the Bay of Begal and south Indian Ocean.

Latent heat flux. The distribution of LHF difference fields between the extreme categories of the summer monsoon over India along with their corresponding statistically significant *t*-value distributions for the pre-monsoon, monsoon, and post-monsoon seasons are depicted in Figure 5.

A zone of significant positive LHF difference of about 20–30 W m^{-2} is observed over the south-western Arabian Sea and adjoining equatorial region during the pre-monsoon season (Figure 5(a)). Such a significant increase in the LHF in this season is caused mainly by the prevailing strong surface winds prior to a flood monsoon season (Mohanty *et al.*, 1994). The increased intensity of the surface wind enhances the turbulent transfer of moisture and frictional convergence at the oceanic surface, resulting in a significant positive LHF anomaly. In addition, a few more small pockets of significant positive LHF differences are observed over the south-eastern Indian ocean.

During the monsoon season (Figure 5(b)), significant positive LHF difference zones are found over the north-east Arabian Sea and the oceanic region adjoining Madagascar in the south Indian ocean. Small pockets of positive/negative LHF differences are also observed over the north Bay of Bengal and central Arabian Sea, but these zones do not attain the desired level of statistical significance. Also, a few negative

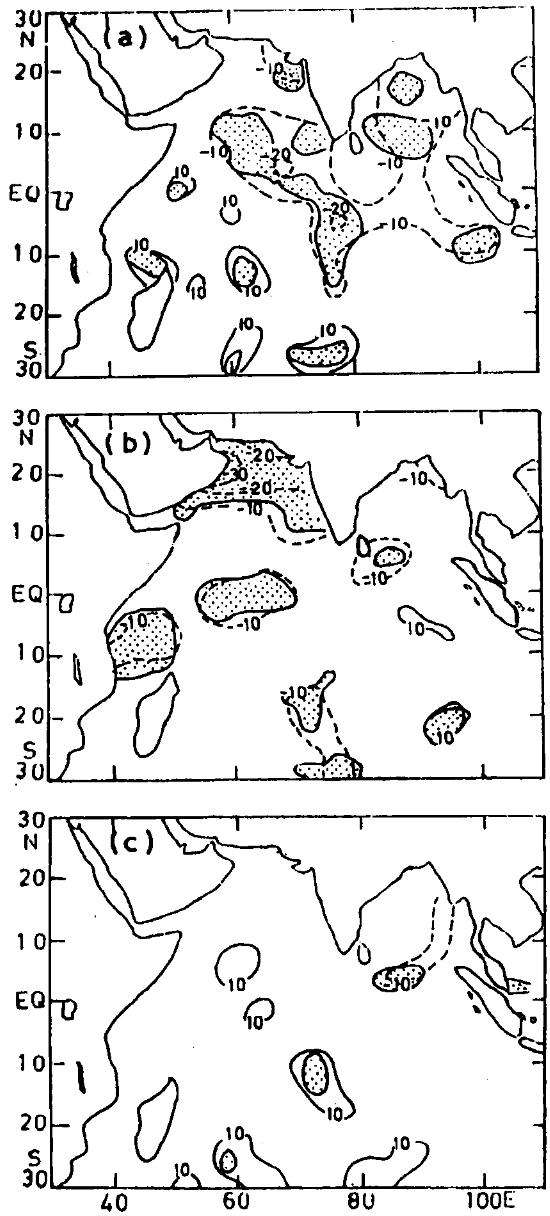

Figure 4. Distribution of incoming shortwave flux anomalies over the Indian seas between the two extreme categories of the summer monsoon (flood/drought). (a) Pre-monsoon; (b) monsoon; (c) post-monsoon. (Isopleth interval: 10 W m^{-2}.) Regions of statistical significance (t-distribution) with confidence limit above 95 per cent are shaded

LHF anomaly zones are observed over the south-east Indian ocean during the monsoon season. It is interesting to note that over the south-east Indian Ocean, the entire positive significant anomaly zone of LHF during the pre-monsoon period changes over to the negative significant anomaly zone during the summer monsoon season. During the pre-monsoon period, trade wind circulation over the south Indian Ocean is quite intense and plays a dominant role in the building up of the cross-equatorial flow over the Bay of Bengal and the Arabian Sea. With the onset of the monsoon, all the intense activity, such as easterly waves and tropical disturbances, which prevail over the oceanic region subsides. Further, the studies of Johri and

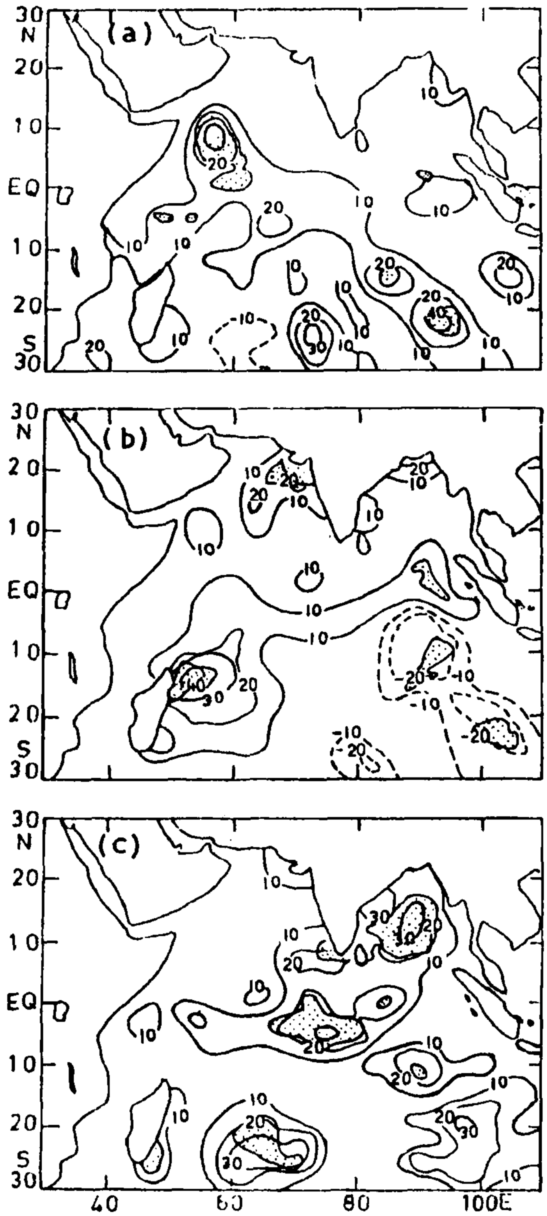

Figure 5. Same as Figure 4 but for latent heat flux (isopleth interval: 10 W m^{-2})

Prasad (1990) have confirmed that there exists an inverse relationship btween the intensity of the convective activity (cloudiness) over the southern hemispheric equatorial trough region (10°S–20°S; 60°E–100°E) and the summer monsoon activity during severe drought momentum years over the Indian subcontinent.

A significant positive LHF difference between the extreme categories of the monsoon (Figure 5(c)) during the post-monsoon season is found over the central and south Bay of Bengal. Usually during this season, synoptic-scale activity, such as easterly waves and tropical disturbances, prevail over the oceanic sectors of the Bay of Bengal. Two zones of significant positive LHF difference, over the central equatorial sectors and over the south Indian Ocean (both of 20 W m^{-2}), are also observed in the post-monsoon season.

Net oceanic heat flux. The difference fields of NHF between the flood and drough monsoon categories, along with their statistically significant *t*-value distributions for the pre-monsoon, monsoon, and post-monsoon seasons, are illustrated in Figure 6.

Distributions of the NHF differences during the pre-monsoon season are dominated by significant net heat loss over the north-east Arabian Sea, south-west Arabian Sea, and adjoining equatorial Indian Ocean prior to a flood monsoon season (Figure 6(a)). In general, these zones are found to be under the influence of a large reduction of SWF and enhancement of LHF in this season. Several pockets of positive NHF anomalies are also found over the Bay of Bengal and south Indian Ocean, but they do not seem to attain the desired level of statistical significance.

Consistent with the reduction of SWF together with the increase in LHF during the summer monsoon season, significant heat-loss regions (negative NHF difference) are observed over the northern and eastern parts of the Arabian Sea and the oceanic area adjoining Madagascar (Figure 6(b)). During the post-monsoon season (Figure 6(c)), significant zones of negative NHF differences are found over the Bay of Bengal, the south-east Arabian Sea, and the central equatorial oceanic region. Incidentally, these regions of excessive heat loss are also characterized by enhanced LHF during the post-monsoon season (Figure 5(c)).

Among the 30 monsoon seasons considered in this study, the monsoon of the year 1961 is categorized as the most excessive monsoon rainfall season, with an excess rainfall of 22·3 per cent above the seasonal mean, and the monsoon of 1972 is categorized as the most deficient monsoon rainfall season, with a deficiency of rainfall of 21·6 per cent below the seasonal mean. In view of the extreme nature of the monsoon behaviour during the years 1961 and 1972, it will be of interest to examine the various components of the oceanic heat budget over the Indian seas during different seasons.

The difference fields of the SWF, LHF, and NHF in the pre-monsoon, monsoon, and post-monsoon seasons between the most extreme years of the summer monsoon activity (1961 and 1972) over India are presented in Figures 7–9. In the pre-monsoon season, large negative SWF differences (exceeding 40 W m^{-2}) are observed over the south Arabian Sea and adjoining equatorial oceanic region, and also over the oceanic region adjoining Madagascar in the west Indian Ocean. Many zones of negative/positive differences of smaller magnitudes are also observed over the Bay of Bengal and the south Indian Ocean. During the monsoon season, the maximum negative flux differences are found over the north and east Arabian Sea. Another zone of large negative SWF difference also lies over the oceanic region off Madagascar and east Africa, and such a feature exists even in the post-monsoon season. On the other hand, a zone of large positive SWF difference found initially in the pre-monsoon season over the south Indian Ocean (10°S, 90°E) is amplified further in the monsoon season and extended over the north-east Indian Ocean as the season extends into the post-monsoon phase.

From the difference fields of LHF between the two years of the most extreme monsoon rainfall activity over India (Figure 8), zones of large positive LHF differences are observed over the Arabian Sea and the Bay of Bengal. The large positive LHF difference zone observed during the pre-monsoon season over the south-west Arabian Sea and adjoining equatorial Indian Ocean shifts northward and lies over the central Arabian Sea during the summer monsoon season. Over the Bay of Bengal also, a zone of large positive LHF anomaly is observed in both the pre-monsoon and monsoon seasons. During the post-monsoon season, large positive LHF difference zones are observed over the Bay of Bengal and the equatorial oceanic sectors. Apart from this, few other zones of large positive and negative LHF difference zones are observed over the south Indian Ocean in all the three seasons.

The difference fields of the NHF between the two most extreme monsoon years (1961 and 1972) during the pre-monsoon season is characterized by a net heat loss all over the oceanic region considered in this study (Figure 9(a)), with larger magnitudes of heat loss found over the south-western Indian Ocean north of Madagascar, south-western Arabian Sea, Bay of Bengal, etc. With the establishment of the monsoon season, the zone of large negative NHF difference found over the south-western Arabian Sea shifts northward. At the same time, the magnitude of net heat loss from the Bay of Bengal is found to intensify further. It is interesting to observe the large heat loss region surrounding Madagascar in the south Indian Ocean during monsoon and post-monsoon seasons, although with reduced magnitudes of oceanic heat loss.

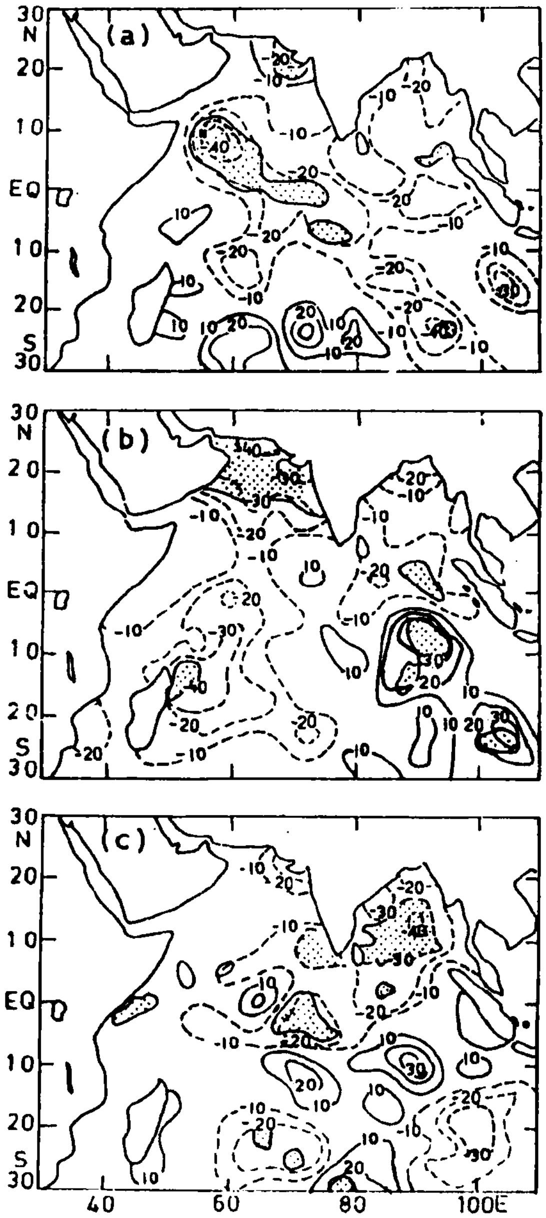

Figure 6. Same as Figure 5 but for net oceanic heat flux (isopleth interval: 10 W m^{-2})

Monthly variations of dominant oceanic heat budget components in flood and drought monsoon years

Monthly variation of SWF, LHF, and NHF during flood monsoon and drought monsoon years are studied over three oceanic sectors, namely equatorial Indian Ocean, Arabian Sea, and Bay of Bengal, where significant flux differences are observed between the extreme categories of the monsoon. The geographical boundaries of these oceanic sectors, as shown in Figure 10, are given below:

(i) west equatorial Indian ocean (box 1), 10·5°S–10·5°N; 53·5°E–67·5°;
(ii) Arabian Sea (box 2), 10·5°N–24·5°N; 55·5°E–75·5°E;
(iii) Bay of Bengal (box 3), 10·5°N–24·5°N; 80·5°E–97·5°E.

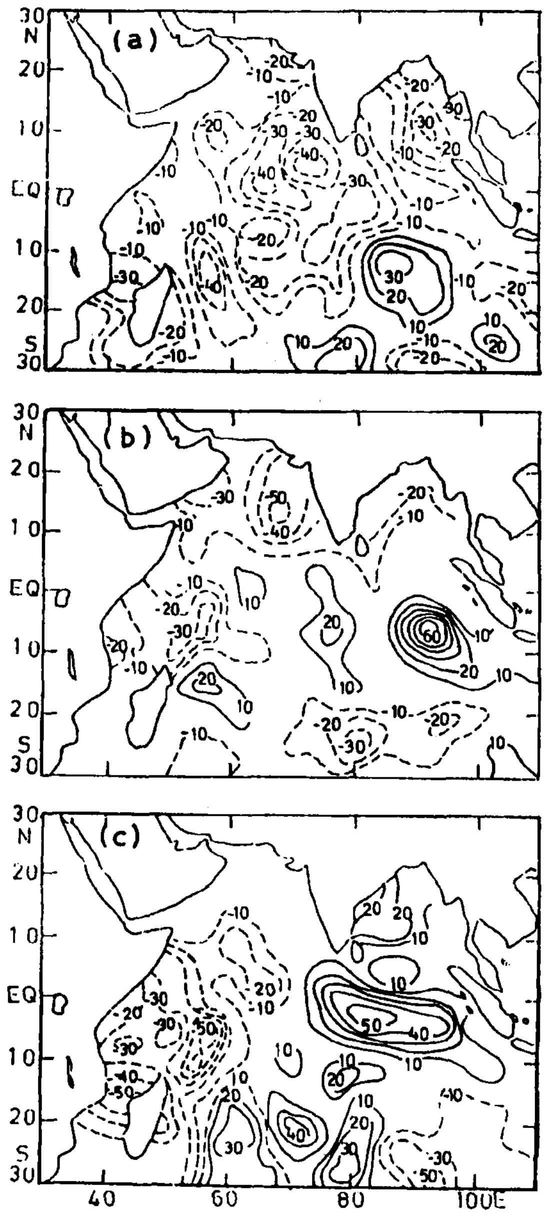

Figure 7. Distribution of incoming shortwave radiation flux anomalies between the year of most excess rainfall (1961) and year of most deficient rainfall (1972). (a) Pre-monsoon; (b) monsoon; (c) post-monsoon. (Isopleth interval: 10 W m^{-2})

Mean monthly values of SWF, LHF, and NHF over box 1, box 2, and box 3 are presented in Figures 11–13. Over box 1, incoming SWF increases from January to March and then decreases sharply during the April–May period. Subsequently, until July, the mean SWF received over box 1 remains nearly the same. Thereafter, a gradual increase of SWF is observed until October, which is followed by a decrease until December. It is interesting to note that during the summer monsoon months (June–September), there is less SWF over box-1 in flood monsoon years. Nearly similar variations of SWF are observed over box 2 (Arabian Sea). However, a general increase of SWF occurs in this box from January to April, and subsequently a gradual decrease is observed until July. Over the Bay of Bengal (box 3), the variation of SWF is the same as that of the equatorial Indian Ocean (box 1) until March, and the subsequent decrease is

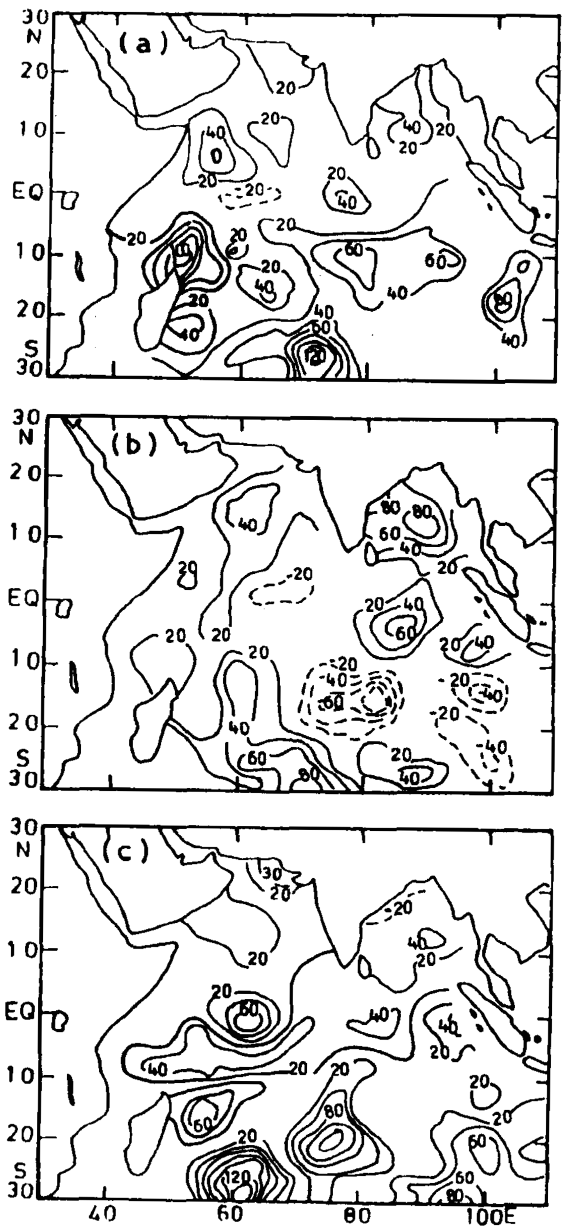

Figure 8. Same as Figure 7 but for latent heat flux (isopleth interval: 20 W m^{-2})

gradual and continues up to June. Beyond June, the observed variations of SWF over box 3 remain more or less unchanged.

In general, the mean monthly variations of LHF are found to be of opposite nature to that of SWF. An important observation of the LHF variations in all three boxes is that of a spectacular increase in its magnitude during the period April–June, and the increase during this period is also found to be more in the case of the flood category of the summer monsoon. Further, the magnitude of increase is found to be more over the equatorial Indian Ocean and the Arabian Sea (maximum) and less over the Bay of Bengal. A characteristic feature is that the increase of LHF from April to May is at its maximum over the equatorial Indian Ocean (box 1) and the Bay of Bengal (box 3), whereas over the Arabian Sea (box 2) the increase in LHF magnitude is found to be at its maximum from May to June. The large increase of LHF observed

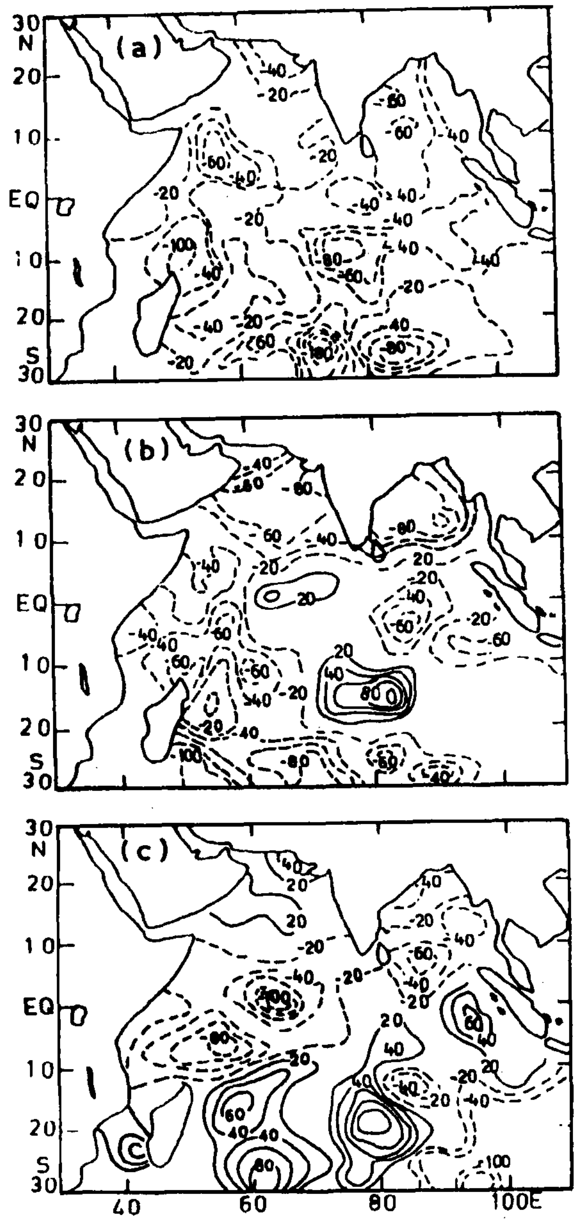

Figure 9. Same as Figure 8 but for net oceanic heat flux (isopleth interval: 20 W m^{-2})

during April–May over box 1 and box 3 may be attributed to the building up of the much stronger monsoon flows prior to a flood monsoon, but the delayed increase of LHF magnitude over the Arabian Sea during May–June could be due to the delay in the progress of the summer monsoon circulation over this area as compared with the equatorial Indian Ocean and Bay of Bengal. After June, a general decrease of LHF is observed until October, which is followed by an increase until December. This reduction of LHF over box 1 and box 2 is found to be dramatic, but such a feature over box 3 is found to be gradual during June–September and is pronounced until October.

The net oceanic heat flux variation shows nearly an opposite feature to that of LHF. The NHF over the ocean reflects mainly a balance between SWF and LHF. A positive NHF (heat gain) implies the dominance of incoming SWF over the LHF, whereas the reverse is true for negative NHF (heat loss). It may be seen from Figures 11–13 that there is a large reduction of NHF (transformation from net heat gain to net heat

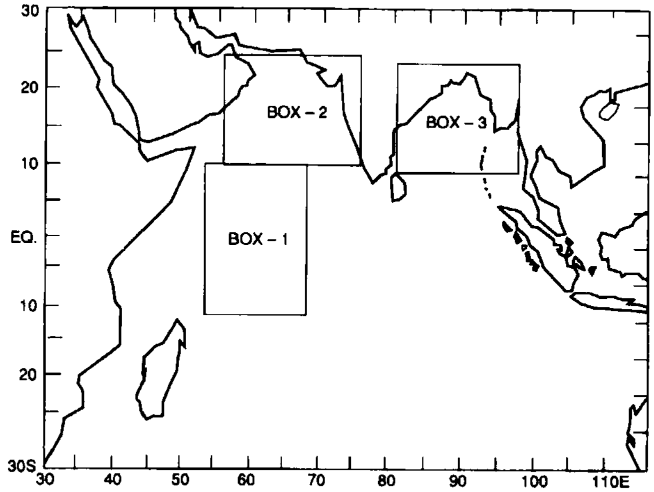

Figure 10. Geographical boundaries of three oceanic sectors. Box 1: west equatorial Indian Ocean. Box 2: Arabian Sea. Box 3: Bay of Bengal over Indian seas

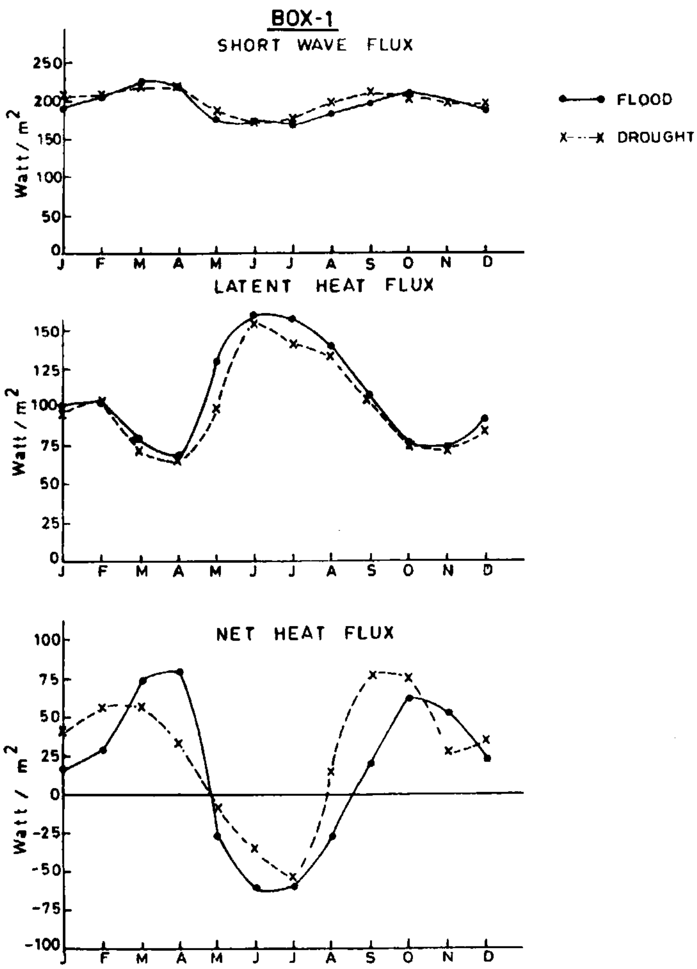

Figure 11. Mean monthly variations of oceanic heat budget components over the west equatorial Indian Ocean (box 1) during extreme categories of summer monsoon (flood and drought) over India. (a) Shortwave flux; (b) latent heat flux; (c) net oceanic heat flux (Units: W m^{-2})

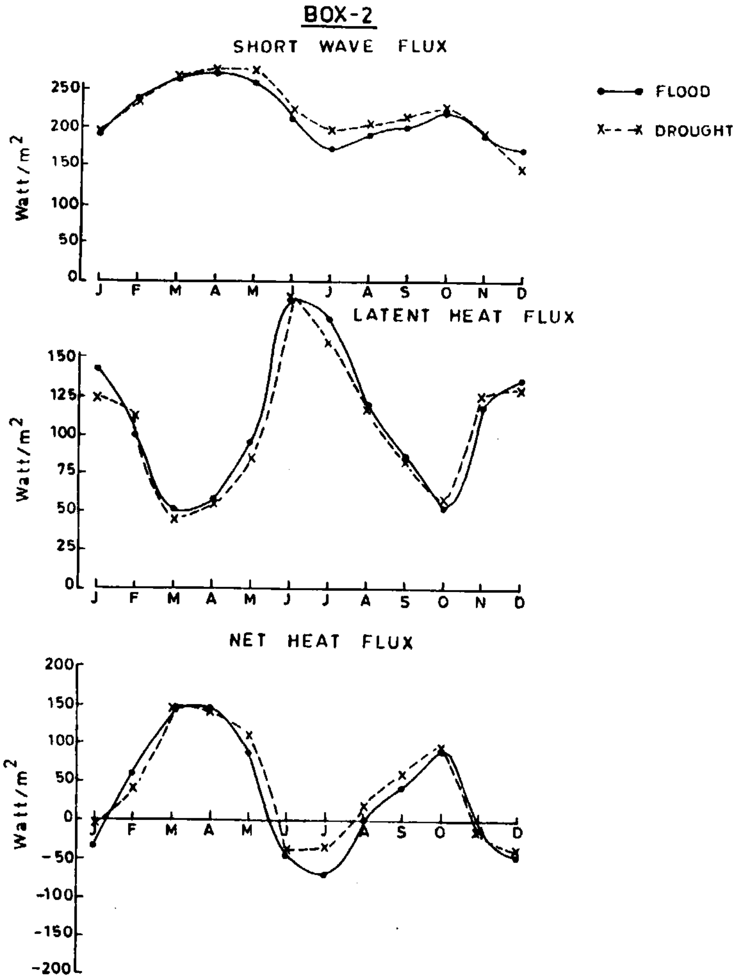

Figure 12. Same as Figure 11 but for Arabian Sea (box 2) (units: W m^{-2})

loss regime) over box 1 and box 3 from April to May in flood monsoon years, which is due mainly to the reduction of SWF and spectacular enhancement of the LHF over these oceanic regions prior to a flood monsoon season over India. Such a feature of net heat loss, however, continues until August over box 1, whereas it continues until September over box 2. It is important to note that over these oceanic sectors of west equatorial Indian Ocean and Bay of Bengal, the magnitude of NHF is much less in the case of the flood category of the monsoon during the month of May and June. However, over the Arabian Sea (box 2), such a large reduction of NHF takes place from May to June in both the categories of the monsoon activity and a net heat loss from the ocean surface is observed during the months of June and July.

In order to examine the NHF variation over these boxes further during the years of most extreme behaviour of the summer monsoon activity, the variations of NHF during the years of 1961 and 1972 are presented in Figure 14. It is found that a large reduction of NHF (transformation from net heat gain to net heat loss regime) takes place over box 1 and box 3 from April to May during the year of most excess monsoon rainfall. Such a feature appears simultaneously over the equatorial Indian Ocean (box 1) and the Bay of Bengal (box 3), owing to the fact that the monsoon current establishes almost at the same time over these oceanic sectors. Further, the appearance of a large reduction in the NHF during the period April–May demonstrates that prior to a flood monsoon the oceanic sectors of box 1 and box 3 experience a spectacular increase of LHF and a reduction of SWF leading to the sharp reduction of NHF. However,

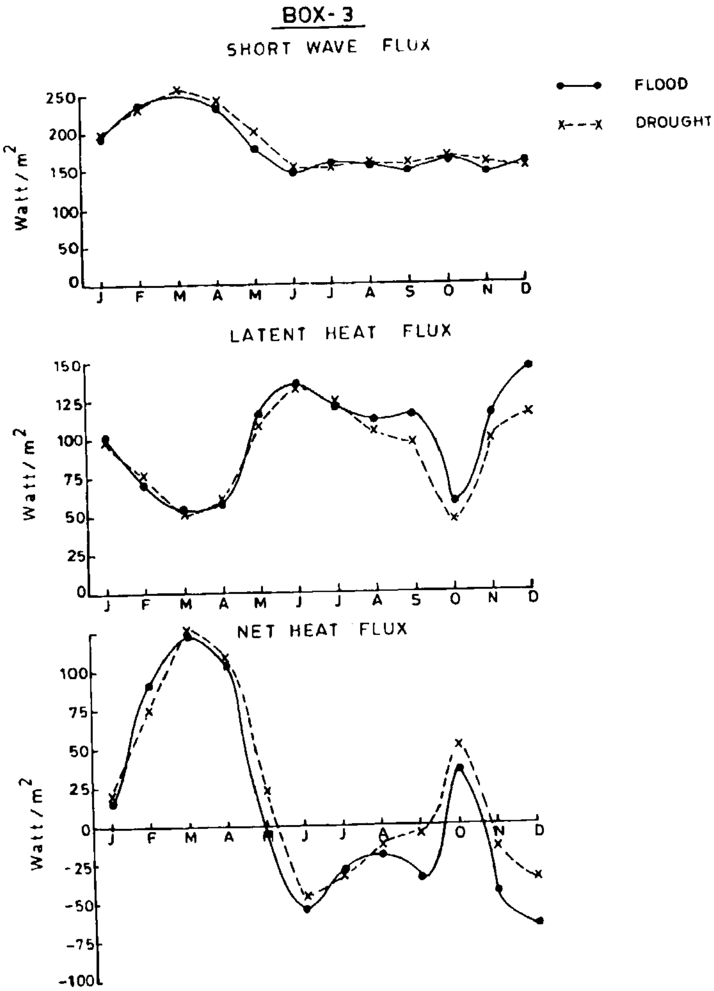

Figure 13. Same as Figure 11 but for Bay of Bengal (box 3) (units: W m^{-2})

such a feature is more prominent over the equatorial Indian Ocean (box 1). The characteristic feature of a decrease in the NHF leading to net heat loss in the year of the most excess rainfall, 1961, however, continues until August over box 1, whereas it continues until September over box 3. Instead, over the Arabian Sea (box 2), a large reduction of NHF takes place during the period May–June as the monsoon current is established only after covering the oceanic regions of box 1 and box 3.

Mean monthly variations of NHF anomalies between the flood and drought monsoon years over the three boxes are presented in Figure 15. Primarily a large negative difference of NHF is found during the month of May, but is found to be at a minimum (very small value) during June in box 1 and box 2 and during July in box 3.

CONCLUSIONS

Based on the results discussed above, the following general conclusions may be drawn.

The mean SWF distribution over the Indian seas in different seasons over India is determined largely by the sun's position and the cloud cover variations over the oceanic areas. The LHF is found to vary considerably over the Arabian Sea, having the maximum flux during the monsoon season and minimum during the pre-monsoon season. During the monsoon season, however, due to the dominance of the LHF over SWF, a zone of net oceanic heat loss is found over the central parts of the Arabian Sea, which

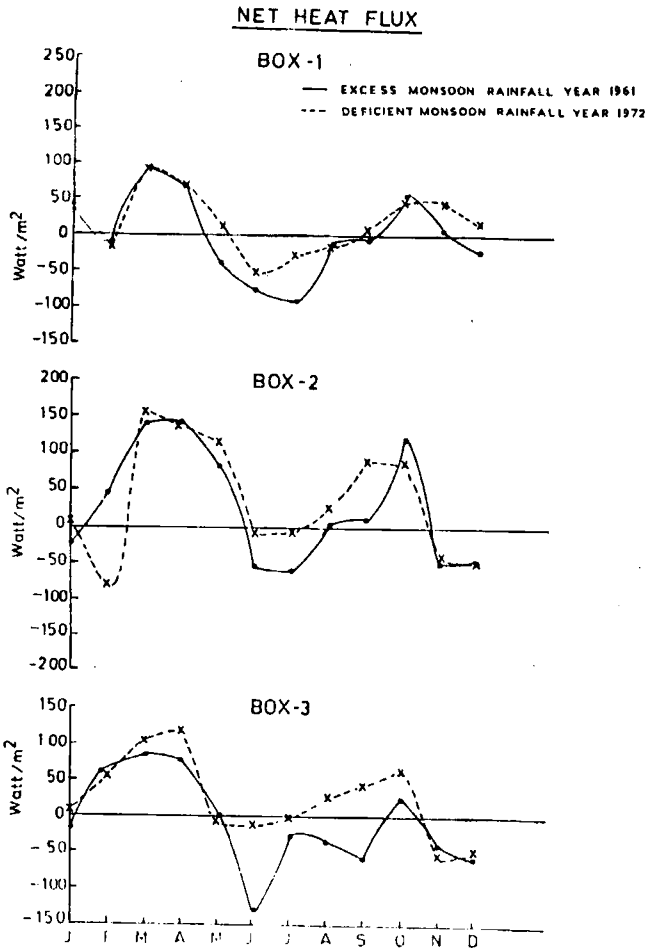

Figure 14. Mean monthly variations of net oceanic heat flux during the year of most excess rainfall (1961) and year of most deficient rainfall (1972) over India. (a) West equatorial Indian Ocean (box 1); (b) Arabian Sea (box 2); (c) Bay of Bengal (box 3) (units: W m^{-2})

produces a positive feedback for the maintenance of deep cumulus convection through the intense turbulent flux transport of heat and moisture to the overlying atmosphere. These flux quantities are transported further upwards through the boundary layer processes, which subsequently provides the necessary moisture for sustaining deep cumulus convection.

The oceanic heat budget components over the Indian seas exhibit significant variability between the two extreme categories of the monsoon over India (flood and drought) during the pre-monsoon season. The dominant feature of the pre-monsoon characteristics of the oceanic heat budget is the increase of cloud cover (with a reduction of SWF) together with the spectacular increase of LHF (with an increase of surface wind) leading to the net heat loss from the oceanic sectors of the equatorial Indian Ocean, south Arabian Sea and the Bay of Bengal.

Mean monthly variations of the oceanic heat budget components over the three selected oceanic regions of the Indian seas exhibit dramatic flux differences between the two extreme categories of the monsoon. It is found that a large reduction of NHF takes place over the west equatorial Indian Ocean and the Bay of Bengal from April to May, and from May to June over the Arabian Sea during the year of most excess rainfall (flood). This indicates that these oceanic sectors experience a dramatic increase of LHF and a reduction of SWF, leading to a sharp reduction of NHF prior to a flood monsoon season over India.

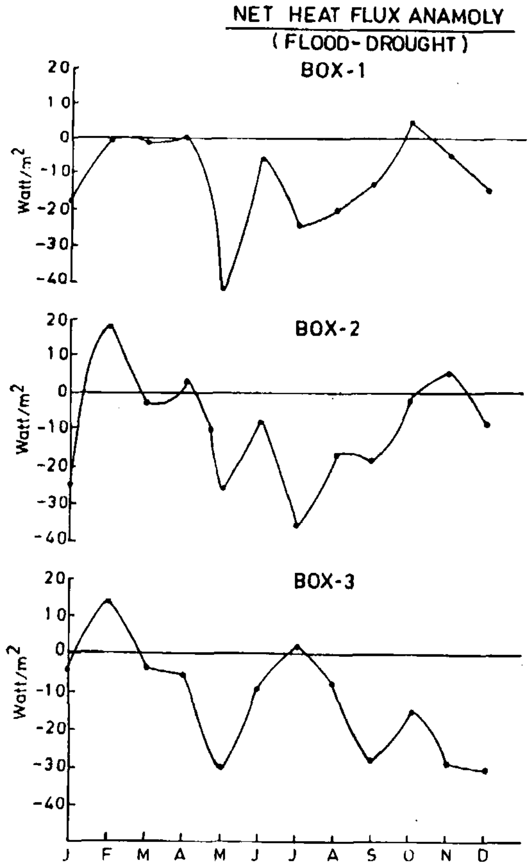

Figure 15. Same as Figure 14 but for the net oceanic heat flux anomalies between the extreme categories of summer monsoon over India (units: W m^{-2})

Thus, this study emphasizes the need for augmentation of marine surface meteorological parameters on a regular basis with the help of sophisticated remote sensing algorithms over the Indian seas. Such efforts would go a long way in enhancing our understanding of the air–sea exchange processes and their role on the monsoon variability.

ACKNOWLEDGEMENTS

We are indeed grateful to Professor A. H. Oort of the Climate Dynamics Group of the Geophysical Fluid Dynamics Laboratory (GFDL), Princeton University, New Jersey, USA for providing the analysed Comprehensive Ocean Atmospheric Data Sets (COADS) used in this study.

APPENDIX

Oceanic heat budget computation

The net oceanic heat budget equation (in W m^{-2}) can be written as

$$Q_N = Q_R - Q_B - Q_H - Q_E \tag{A1}$$

Estimation of incoming solar radiative flux (Q_R). Q_0 is computed as a function of geographical and astronomical factors, such as latitude of the place and time of the year, following Seckel and Beaudry

(1973), in the following manner:

$$Q_0 = A_0 + A_1 \cos(\phi) + B_1 \sin(\phi) + A_2 \cos(2\phi) + B_2 \sin(2\phi)$$

where

$$A_0 = -15{\cdot}82 + 326{\cdot}87 \cos(L)$$
$$A_1 = 9{\cdot}63 + 192{\cdot}44 \cos(L + \pi/2)$$
$$A_2 = -0{\cdot}64 + 2 \times 7{\cdot}80 \sin(L - \Pi/4) \cos(L - \Pi/4)$$
$$B_1 = -3{\cdot}27 + 108{\cdot}70 \sin(L)$$
$$B_2 = -0{\cdot}50 + 14{\cdot}42 \cos(2(L - \Pi/36))$$
$$\phi = (JD - 21) \times 360/365 \text{ (in radians)}$$

where JD is the Julian day and L is the latitude of a place (in radians).

Variable Q_0 (W m^{-2}) is then corrected for the transmission of radiation through clouds and noon altitude of the sun, following Reed (1977).

$$Q_R = Q_0(1 - 0{\cdot}62C + 0{\cdot}0019H)(1 - A) \quad \text{(A2)}$$

where C is the cloud amount, H is the noon altitude of the sun in degrees, and A is the albedo of the sea surface. The noon altitude of the sun is obtained as

$$\sin(H) = \sin(L)\sin(d) + \cos(L)\cos(d) \quad \text{(A3)}$$

where L is the latitude of a place and d is the declination of the sun. The declination of the sun is obtained as a function of Julian day (JD) in the following manner

$$d = -23{\cdot}45 \cos(T)$$

where

$$T = (JD \times 360)/365 \quad \text{(in radians)}$$

The albedo of the sea surface (A) is a function of month and latitude is estimated following Payne (1972).

Estimation of effective outgoing longwave radiation (Q_B). In general, the effective outgoing longwave radiation flux does not exhibit much temporal and spatial variability and is a very small quantity over the tropical seas. It is parameterized following the method of Giruduk and Malevski-Holekyich (1973), which is found to give least errors in the computation of Q_{BR} during the south-west monsoon season over the Indian Seas (Mohanty, 1981; Mohanty and Mohan Kumar, 1991).

Based on the special actinometric observations collected during the Indo-Soviet Monsoon Experiments during MONSOON-77 and MONEX-79, the systematic errors in the estimation of longwave radiative flux are reduced between the computed values of Q_{BR} and the measured values by establishing a statistical relationship (Mohanty and Mohan Kumar, 1990) as given below

$$Q_B = 0{\cdot}0308 + 0{\cdot}3174\, Q_{BR} \quad \text{(A4)}$$

The small values in the regression coefficients in equation (A4) suggest that Q_{BR} is very close to Q_B and thus the empirical relationship used for the estimation of Q_{BR} are fairly accurate. However, considerable reduction of systematic errors in the estimation of longwave flux can be achieved through the use of equation (A4) to overcome certain inadequacies in the surface observations (Mohanty and Mohan Kumar, 1991).

Estimation of sensible and latent heat fluxes (Q_H *and* Q_E). The sensible and latent heat fluxes are computed based on the bulk aerodynamic formulation, where the fluxes are parameterized in terms of moisture and temperature gradients and wind velocity at the surface of the MBL. The latent heat flux (Q_E) is given by

$$Q_E = \rho L C_E U[q(T_s) - q_a] \tag{A5}$$

and the sensible heat exchange across the air–sea interface is expressed as

$$Q_H = \rho C_P C_H U[T_s - T_a] \tag{A6}$$

In this study, both the exchange coefficients C_E and C_H are assumed to be the same. For their computation, the following formulations based on wind speed and atmospheric stability are used (Mohanty and Mohan Kumar, 1990).

For $U < 5$ and $\Delta T < 1$

$$10^3 C_H = 0{\cdot}926 + 0{\cdot}682\Delta T + 0{\cdot}046U - 0{\cdot}093\Delta T^2 + 0{\cdot}00074U^2$$

For $U < 5$ and $1 < \Delta T < 9$

$$10^3 C_H = 1{\cdot}751 + 0{\cdot}102\Delta T - 0{\cdot}157U - 0{\cdot}007\Delta TU - 0{\cdot}003\Delta T^2 + 0{\cdot}011U^2$$

For $5 < U < 9$ and $1 < \Delta T < 9$

$$10^3 C_H = 1{\cdot}085 + 0{\cdot}145\Delta T - 0{\cdot}007U$$

For $9 < U < 15$ and $1 < \Delta T < 9$

$$10^3 C_H = 1{\cdot}03 + 0{\cdot}067\Delta T + 0{\cdot}025U - 0{\cdot}003\Delta TU - 0{\cdot}002\Delta T^2 - 0{\cdot}00021U^2$$

where U is the wind speed, ΔT is the effective temperature expressed as

$$(T_s - T_a)(1 + 0{\cdot}07/\mathrm{B})$$

which gives a measure of atmospheric stability, B is the Bowen's ratio given by

$$B = C_P P(T_s - T_a)/0{\cdot}622L(e_s - e_a)$$

REFERENCES

Bhalme, H. N. and Jadhav, S. K. 1984. 'The southern oscillation and its relation to the monsoon rainfall', *J. Climatol.*, **4**, 509–520.

Bunker, A. F. 1976. 'Computations of surface energy flux and annual air–sea interaction cycles of the north Atlantic Ocean', *Mon. Wea. Rev.*, **104**, 1122–1140.

Das, P. K. 1983. *IMO Monograph on Monsoons*, Fifth IMO Lecture Series, World Meteorological Organization, Geneva, 155 pp.

Egorov, B. N. 1976. *Tropex-74*, Hydrometeorological Publisher, Leningrad, pp. 594–599.

Fletcher, J. O., Slutz, R. J. and Woodruff, S. D. 1983. 'Towards a comprehensive ocean atmosphere data set', *Trop. Ocean Atmos. News Lett.*, **20**, 13–14.

Giruduk, G. V. and Malevski-Holekyich, S. P. 1973. Trudi Main Geophysical Observations, Leningrad, **297**, 124–132.

Hastenrath, S. and Lamb, P. J. 1979. *Heat Budget Atlas of the Indian Ocean—Part II: Oceanic Heat Budget*, University of Wisconsin Press, 110 pp.

Johri, A. P. and Prasad, O. 1990. 'Interaction of southern hemispheric equatorial trough with the southwest monsoon circulation during severe drought years', *MAUSAM*, **41**(4), 597–602.

Kondo, J. and Akira Mirua 1985. 'Surface heat budget of the south western Pacific for May 1979', *J. Meteorol. Soc. Jpn*, **63**, 633–646.

Manabe, S., Bryan, K. and Spelman, M. J. 1975. 'A global ocean atmospheric climate model. Part I: the atmospheric circulation', *J. Phys. Ocean.*, **5**, 3–29.

Mohanty, U. C. 1981. 'Estimation of effective long-wave radiation from the Bay of Bengal', *MAUSAM*, **32**(1), 11–16.

Mohanty, U. C., Dube, S. K. and Singh, M. P. 1983. 'A study of heat and moisture budget over the Arabian Sea and their role in the onset and maintenance of summer monsoon', *J. Meteorol. Soc. Jpn*, **61**, 208–221.

Mohanty, U. C. and Mohan Kumar, N. 1990. 'A study of surface marine boundary layer fluxes over the Indian seas during different epochs of Asian summer monsoon', *Atmos. Environ.*, **24A**, 823–828.

Mohanty, U. C. and Mohan Kumar, N. 1991. 'A method of estimation of long-wave radiation over the Indian seas based on surface synoptic observations', *MAUSAM*, **42**(4), 375–380.

Mohanty, U. C. and Ramesh, K. J. 1993. 'Characteristics of certain surface meteorological parameters in relation to the interannual variability of Indian summer monsoon', *Proc. Indian Acad. Sci. (Earth Plan. Sci.)*, **102**(1), 73–87.

Mohanty, U. C., Ramesh, K. J., Mohan Kumar, N. and Potty, K. V. J. 1994. 'Variability of the Indian summer monsoon in relation to oceanic heat budget over the Indian seas', *Dyn. Atmos. Oceans*, **21**, 1–22.

Oort, A. H., Pan, Y. H., Reynolds, R. W. and Popelewski, C. F. 1987. 'Historical trends in the surface temperature over the oceans based on COADS', *Climate Dyn.*, **2**, 29–36.

Payne, R. E. 1972. 'Albedo on the sea surface', *J. Atmos. Sci.*, **29**, 959–970.

Pisharoty, P. R. 1965. 'Evaporation from the Arabian Sea and Indian south west monsoon', in Pisharoty, P. R. (ed.), *Proceedings of International Indian Ocean Expedition*, pp. 43–54.

Rao, K. G. and Goswamy, B. N. 1988. 'Interannual variations of the SST over the Arabian Sea and the Indian monsoon: a new perspective', *Mon. Wea. Rev.*, **116**, 558–568.

Reed, R. K. 1977. 'On estimating insolation over the ocean', *J. Phys. Ocean.*, **7**, 482–485.

Seckel, G. R. and Beaudry, F. H. 1973. 'The radiation from Sun and sky over the north Pacific Ocean (abstract)', *Trans. Am. Geophys. Union*, **54**, 1114.

Shukla, J. 1975. 'Effects of Arabian Sea surface temperature anomaly on Indian monsoon: a numerical experiment with GFDL model', *J. Atmos. Sci.*, **33**, 503–511.

Shukla, J. 1987. 'Interannual variability of monsoons', in Fein, J. S. and Stephens, P. (eds), *Monsoons*, Wiley, Chichester.

Weare, B. C. 1979. 'A statistical study of the relationships between ocean surface temperatures and the Indian monsoon', *J. Atmos. Sci.*, **36**, 2279–2291.